Published in final edited form as:
J Am Soc Mass Spectrom. 2011 August ; 22(8): 1409–1419. doi:10.1007/s13361-011-0150-8.

Reagent Precoated Targets for Rapid In-Tissue Derivatization of the Anti-Tuberculosis Drug Isoniazid Followed by MALDI Imaging Mass Spectrometry

M. Lisa Manier[1], **Michelle L. Reyzer**[1], **Anne Goh**[2], **Veronique Dartois**[2], **Laura E. Via**[3], **Clifton E. Barry III**[3], and **Richard M. Caprioli**[1,4]

[1]Mass Spectrometry Research Center, Vanderbilt University, Nashville, Tennessee, USA

[2]Novartis Institute for Tropical Diseases, Biopolis, Singapore

[3]National Institute of Allergy and Infectious Diseases, National Institutes of Health, Bethesda, Maryland, USA

[4]Departments of Chemistry, Pharmacology, and Biochemistry, Vanderbilt University School of Medicine, 465 21st Avenue South, Medical Research Building 3, Room 9160, Nashville, TN 37232–8575, USA

Abstract

Isoniazid (INH) is an important component of front-line anti-tuberculosis therapy with good serum pharmacokinetics but unknown ability to penetrate tuberculous lesions. However, endogenous background interferences hinder our ability to directly analyze INH in tissues. Chemical derivatization has been successfully used to measure isoniazid directly from tissue samples using matrix-assisted laser desorption/ionization (MALDI) imaging mass spectrometry (IMS). MALDI targets were pretreated with *trans*-cinnamaldehyde (CA) prior to mounting tissue slices. Isoniazid present in the tissues was efficiently derivatized and the INH-CA product measured by MS/MS. Precoating of MALDI targets allows the tissues to be directly thaw-mounted and derivatized, thus simplifying the preparation. A time-course series of tissues from tuberculosis infected/INH dosed animals were assayed and the MALDI MS/MS response correlates well with the amount of INH determined to be in the tissues by high-performance liquid chromatography (HPLC)-MS/MS.

Keywords

Matrix-assisted laser desorption/ionization; Imaging mass spectrometry; Isoniazid; Tuberculosis; *trans*-cinnamaldehyde; Derivatization; Precoated MALDI targets

Introduction

Since the introduction of matrix-assisted laser desorption/ionization (MALDI)-based imaging mass spectrometry [1], this technology has been used to study the spatial localization of a variety of analytes directly from thin tissue sections, including proteins [2–4], peptides [5, 6], lipids [7–9], and small xenobiotics [10–12]. The advantages of imaging with MALDI mass spectrometry are numerous, including simple sample preparation, high sensitivity (attomole/femtomole range for many compounds), and relatively fast sampling speeds (up to 100 ms/pixel, depending on desired resolution and sensitivity). Imaging mass

Correspondence to: Richard Caprioli; r.caprioli@vanderbilt.edu.

spectrometry (IMS) allows an assessment of local drug concentrations in situ within the lesions of infected animals and therefore adds highly valuable information to simple serum pharmacokinetic analyses.

While MALDI IMS is becoming increasingly popular for the analysis of drugs and metabolites within tissue sections, it can be challenging due to low molecular weight background signals. Endogenous species that may produce spectral interferences and/or contribute to ionization suppression are routinely removed from tissues using washing protocols prior to protein analysis [13–16] (for example, successive washes in graded ethanol solutions remove salts and most lipids); however, this approach may extract or delocalize small molecule analytes as well. Other approaches to overcome these interferences have involved the selective choice of MALDI matrix [17], the use of high-resolution FT-MS analysis [18], or MS/MS analysis [9, 11, 12].

In cases where compounds exhibit poor ionization efficiency, chemical derivatization may be employed to increase ion yields. Chemical derivatization [19, 20] is routinely used to improve detection of drugs by a variety of analytical techniques, including gas chromatography (GC), high-performance liquid chromatography (HPLC), and increasingly MALDI MS [21–30]. Recently, this approach has also been used in conjunction with IMS for direct tissue analysis [31]. For example, Franck et al. utilized the reactive (*N*-succinimidyloxycarbonylmethyl)tris(2,4,6-trimethoxyphenyl) phosphonium bromide (TMPP) compound to direct peptide fragmentation towards the N-terminus for in situ tryptic peptides [31].

Adding a derivatization agent to tissue sections complicates the sample preparation process. The derivatization agent may contribute to analyte delocalization, signal suppression, and may interfere with matrix crystal formation. Precoating of MALDI targets has been employed as a strategy to apply matrix to a surface for improved reproducibility or sensitivity. Vorm et al. used fast evaporation of solvent from matrix solutions to produce a thin layer of homogenous microcrystals directly on a MALDI target plate [32]. Regenerated cellulose has been affixed to MALDI plates followed by treatment with α-cyano-4-hydroxycinnamic acid (CHCA) in order to collect continuous effluent from a capillary electrophoresis unit [33]. Similarly, peptides from protein digests were resolved using capillary reversed-phase HPLC and deposited onto CHCA-coated MALDI targets [34]. These precoated targets facilitated off-line coupling of HPLC separation with MALDI analysis, allowing improved sensitivity for low abundance peptides.

More recently, entire MALDI targets were precoated with 2,5-dihydroxybenzoic acid matrix using sublimation. Tissue sections were thaw-mounted onto the precoated targets and directly analyzed by MALDI IMS. This approach resulted in 1–2 μm sized crystals with minimal analyte delocalization as no extraction solvents were applied. Lipids, peptides, and small molecules (drug compounds) were amenable to analysis using this technique [35].

Isoniazid (INH) is widely used in first-line treatment for tuberculosis as part of a four-drug combination therapy. INH is well absorbed and has good pharmacokinetic properties that result in a rapid bactericidal activity on organisms within patients' sputum [36, 37]. Unfortunately this activity is limited to the first month or two of treatment, after which it is thought to have little long-term "sterilizing" activity [38]. Sterilizing activity is a complex phenomenon related to the ability of the drug to prevent relapse with active disease after discontinuing chemotherapy. The poor sterilizing activity of the four drug combination is reflected in the 6–8 mo regimen required to achieve a sterile cure. There are many different theories around the intrinsic sterilizing potential of various drugs [39] but perhaps the most straightforward is related to the ability of drugs to partition out of serum and into the dense

granulomas that form the basis of much of the lung pathology of the disease. To test that theory, we have been exploring IMS as a method to assess the tissue penetration of TB drugs into lesions. Our initial efforts to study INH distribution within tissue sections by MALDI IMS proved difficult due to endogenous tissue interferences. Isoniazid has been derivatized previously using *trans*-cinnamaldehyde [40] and *N*-methyl-9-chloroacridinium triflate [41] to improve its detection by HPLC with ultraviolet/visible (UV/Vis) analysis. It has also been analyzed as the copper chelated Schiff base of salicylaldehyde-5-sulfonate using capillary zone electrophoresis [42].

Here we present an in-tissue chemical derivatization protocol for isoniazid in order to attain suitable sensitivity for imaging analyses of dosed tissue samples using MALDI IMS. We investigated the derivatization of isoniazid under various pH, temperature, time, and solvent conditions using several aldehydes, steroids, and succinimidyl carbamates. The optimal reagent, *trans*-cinnamaldehyde, was then applied to MALDI targets prior to tissue samples and utilized for the analysis of lung tissue sections from tuberculosis infected rabbits treated with a multi-drug mixture containing isoniazid. The reagent precoated targets allow for rapid in-tissue derivatization and thus provide a convenient platform for imaging MS studies where derivatization is required.

Experimental

Materials

The following reagents were purchased from Sigma-Aldrich Chemical Co. (St. Louis, MO, USA) and used for INH derivatization: *trans*-cinnamaldehyde, β-phenylcinnamaldehyde, α-bromocinnamaldehyde, 4-hydroxy-3-methoxycinnamaldehyde, 4-nitrocinnamaldehyde, *trans*-4-(diethylamino) cinnamaldehyde, hydrocortisone, and (*N*-succinimidyloxycarbonylmethyl)tris(2,4,6-trimethoxyphenyl)phosphonium bromide (TMPP). Additionally, Waters AccQ-Fluor derivatizing reagent (6-aminoquinolyl-*N*-hydroxysuccinimidyl carbamate) was purchased from Waters Corporation (Milford, MA, USA). Methanol and acetonitrile (both HPLC grade) were obtained from Fisher Scientific (Pittsburgh, PA). Trifluoroacetic acid (TFA), isoniazid and α-cyano-4-hydroxycinnamic acid (CHCA) were also obtained from Sigma-Aldrich.

Method Development with Derivatization Reagents for MALDI IMS Analysis

Chemical derivatives of isoniazid were formed with the nine different reagents. Parameters were based on those recommended in published methods for derivative reactions of similar compounds [19, 20, 31, 40, 43–45]. For tissue analysis, derivatization reagents were applied by either spray coating, sublimation, or spin coating (detailed below). Based on preliminary data, *trans*-cinnamaldehyde (CA) was chosen for analysis of study samples.

Animal Studies

Experiments utilizing New Zealand White (NZW) rabbits aerosol infected with *M. tuberculosis* as previously described [46] were performed with the approval of the animal care and use committee (ACUC) of NIH/NIAID under assurance #A-4149-01 and protocol #LCID-3. Tuberculosis-infected rabbits were dosed with rifampin/isoniazid/pyrazinamide/moxifloxacin at 30/50/125/25 mg/kg administered orally once daily for 1 wk, then sacrificed at various time points after the final dose. Control rabbits were dosed with rifampin (24 mg/kg). For MALDI analyses, lung regions containing lesions were snap-frozen in vapor phase liquid nitrogen, subjected to 3 Mrad γ radiation as a sterilization procedure, shipped frozen on dry ice, and stored at −80 °C until use.

Tissue Preparation for HPLC-MS/MS Analysis

Drug containing tissues were processed at the time of sacrifice (BSL-3 facility) with the sample preparation procedure described below, and the final lyophilized extracts were shipped for quantitative analysis. This preparation procedure was validated to sterilize the samples prior to shipment. Tissue was homogenized in phosphate buffered saline (PBS) using a Qiagen TissueLyser bead beater (Hilden, North Rhine-Westphalia, Germany), with 1 mL PBS added for every 0.2 g of tissue. Warfarin was added as an internal standard. Proteins were precipitated and INH extracted by addition of acetonitrile with 0.2% acetic acid in a 9:1 ratio of extractant to tissue homogenate. Samples were vortexed for 1 min, centrifuged at 1000 *g* for 10 min, and the supernatant removed. The extracts were lyophilized, shipped on dry ice, and frozen at −20 °C until they were reconstituted in mobile phase and analyzed. Drug free tissue that was infected with *M. tuberculosis* and sterilized via γ irradiation was used as naive material for calibration standards, quality control samples and blanks. Each was spiked with warfarin internal standard, then processed by the procedure used for study samples. Calibration standards ranged from 10.2 ng/mL to 10.4 μg/mL.

Tissue Preparation for MALDI IMS

The frozen tissues were cut at −20 °C into 12-μm thick sections on a cryostat (Leica Microsystems Inc., Bannockburn, IL, USA) and thaw-mounted directly onto gold-coated stainless-steel MALDI target plates (Applied Biosystems, Foster City, CA, USA) or onto target plates precoated with *trans*-cinnamaldehyde. Tissues were analyzed by two different methods: (1) for underivatized INH or (2) for INH derivatized with CA using precoated targets as detailed below. In addition, a serial section of each tissue was cut and mounted on a glass slide and stained with hematoxylin and eosin (H&E) for anatomical visualization.

CHCA was used as the MALDI matrix and was prepared as a 15 mg/mL solution in 60:40 acetonitrile:water (with 0.1% TFA). CHCA was coated over the entire surface of all tissues mounted on MALDI plates. This was accomplished by placing the solution into a thin layer chromatography (TLC) glass reagent sprayer (Kontes Glass Company, Vineland, NJ, USA) and spraying multiple coats at a distance of ~20 cm across the surface of the tissue. One coating cycle consisted of passing the sprayer two times across the surface of the tissue and allowing the tissue to dry. This process was repeated until there was a homogeneous layer of matrix crystals over the surface of the tissue, usually about 5–8 cycles. The plates were desiccated for at least 15 min prior to instrumental analysis.

Pretreatment of MALDI Plates with CA Using High Velocity Spin Coating

In order to create precoated targets, *trans*-cinnamaldehyde was deposited on MALDI target plates using high velocity spin coating. A target was vacuum sealed to the chuck of a WS-400 bench-top single wafer spinner (Laurell Technologies Corporation, North Wales, PA, USA). Approximately 1 mL of 50% CA in methanol was deposited onto the center of the plate and spinning commenced for 10 s at 500 rpm for an initial spread of reagent. The speed was then increased to 2000 rpm for 20 s to form a homogeneous coating of CA. The CA-coated plate was stored overnight in the dark at room temperature to allow crystal formation prior to tissue placement the following day. After tissues were thaw-mounted, the plates were allowed to incubate for at least 30 min at room temperature prior to matrix application as detailed above.

HPLC-MS/MS Analysis

Lyophilized extracts were thawed and reconstituted into 200 μL mobile phase. Ten μL were injected into an HPLC system (Symbiosis Pharma, Spark Systems Solutions, The

Netherlands) and separated at a flow rate of 1 mL/min on a Gemini C6-phenyl 4.6 × 150 mm, 5 μm column (Phenomenex, Torrance, California, USA) held at 35 °C. A gradient elution was used, starting with 97% mobile phase A (water with 0.2% acetic acid) and going to 85% mobile phase B (methanol with 0.2% acetic acid) in 4.5 min. The analysis was performed using an Applied Biosystems/Sciex API4000 triple-quadrupole mass spectrometer (Foster City, California, USA). Selected reaction monitoring (SRM) of precursor-to-product transitions were used in electrospray positive ionization mode to track presence of analytes. Quantitation of drug levels was performed using the *m/z* transitions 309.2→251.1 for warfarin and 138.0→121.1 for isoniazid with collision energies of 28 and 21 eV, respectively. Although rifampin, pyrazinamide, and moxifloxacin were quantified also, results are not presented here. The flow rates of curtain and collision gas were set to 25 and 6 psi, respectively. Ultra pure nitrogen was used with a nebulizing temperature of 500 °C. The ion spray voltage, nebulizing gas (GS1) and Turbo gas (GS2) were set at 5500 V, 45 and 60 psi, respectively. The dwell time for each SRM transition was 100 ms. Compound specific MS parameters were optimized for each analyte. Calibration curve data were evaluated using a quadratic fit and 1/x weighting. Sample analysis was accepted if the low level quality control samples were within ±20% of nominal concentration and ±15% for mid and high level quality control samples.

MALDI Imaging Mass Spectrometry

Mass spectra were acquired in positive-ion mode using a MALDI LTQ XL linear ion trap mass spectrometer (Thermo Scientific, San Jose, CA, USA), equipped with a 337-nm nitrogen laser operating at 60 Hz and resulting in ~40 × 100 μm laser spot size. Dissociation of protonated molecules was achieved using an isolation window of 1 Da and CID energy of 40 for INH or 50 for INH-CA (arbitrary units) with helium as the trapping/collision gas. Isolated precursor ions were activated for 30 ms using an rf frequency activation Q value of 0.5 (INH) or 0.25 (INH-CA). Product ion mass spectra were acquired over the *m/z* range 75–170 (INH) and 65–300 (INH-CA). For MS/MS imaging experiments, an average of 15 laser shots per scan was used to produce a mass spectrum every 200 μm laterally across the tissue. Two dimensional ion density images were extracted from the raw data using ImageQuest ver. 1.0.1 (Thermo Scientific, San Jose, CA, USA).

Results and Discussion

Imaging MS/MS Analysis of Underivatized INH

Analysis of INH by mass spectrometry is straightforward using high-performance liquid chromatography and electrospray ionization [47–51]. However, due to endogenous interfering components at this very low mass range in tissue, the in situ analysis of INH by MALDI has been challenging. Fragmentation of underivatized INH yields predominantly one product ion (*m/z* 138→121) as shown for the standard in Figure 1a (top spectrum). Unfortunately, there is also an endogenous background signal in rabbit lung tissue with the same transition (Figure 1a, control lung spectrum). Due to high background at *m/z* 121 in the lung tissue, it is not possible to easily distinguish control from dosed (1 h 5 min) tissue (Figure 1b), even though this tissue contains a relatively high concentration of INH (approximately 10 μg/g tissue, as determined by HPLC-MS/MS). MS^3 capabilities of the ion trap (*m/z* 138→121→) were also utilized but did not improve the results. Therefore, derivatization of INH in lung tissue was investigated.

Chemical Derivatization of INH

We explored derivatives of INH in solution with each of the reagents listed in Table 1 under various solvent, pH, concentration, temperature, and time conditions following recommended published methods for similar derivative reactions [19, 20, 31, 40, 43–45].

Listed are INH-derivative precursor ions ($[M]^+$ or $[M + H]^+$), predominant MS/MS fragments, derivative-to-INH molar ratios, and reaction parameters. Under the conditions used, some reagents formed derivatives in solution virtually immediately at room temperature (e.g., *trans*-cinnamaldehyde) while others were more easily formed at higher temperatures and elevated pH conditions (TMPP). The most promising derivatization agents were further evaluated on tissue sections and were applied by spray or spin coating or by sublimation [7] as described previously.

Sublimation is an obvious choice to precoat reagent on targets because it forms a very homogeneous coating in a relatively short period of time (5–15 min). While *trans*-cinnamaldehyde provided excellent sensitivity in derivatizing INH, it is a liquid and thus not amenable to sublimation. In addition, MALDI plates coated with CA via spin coating required overnight drying prior to use. Thus, other cinnamaldehyde-based derivatization agents, which are solids at room temperature, were evaluated including β-phenylcinnamaldehyde and 4-hydroxy-3-methoxycinnamaldehyde (Methods section and Table 1). These reagents were precoated onto MALDI targets using sublimation procedures. Uniform solid coatings of reagents were obtained; however derivatization of INH in tissue samples did not occur on the precoated target alone in the absence of added solvent. Thus, the target plates were placed in a chamber containing methanol and acetonitrile vapor at room temperature for 10 min to 1 h in order to wet the tissues and promote INH-derivative formation. Plates were then coated with CHCA matrix. The reproducibility of the INH-derivative signal was not reliable plate-to-plate and, in some instances, no significant signal was obtained above undosed tissue background; therefore no further work was done with these reagents.

Hydrocortisone produced an INH derivative ($[M + H]^+ = 482$) with standard INH, however it was not further evaluated in tissue. The major MS/MS fragments of the INH-hydrocortisone derivative are *m/z* 464 and 452, corresponding to losses of H_2O and CH_2O, respectively. These are not very specific losses and therefore potentially more susceptible to endogenous interferences. Two succinimidyl carbamates were studied, Waters AccQ-Fluor and TMPP, which both formed detectable derivatives with INH in solution. Waters AccQ-Fluor was not evaluated in tissue because the amount of reagent required to coat a target plate was cost-prohibitive. The other, TMPP, forms a derivative with INH that is positively charged and thus readily detected by MS. TMPP was further evaluated with several different modifiers (Table 1) to obtain pH ~8–9, which is optimal for derivatization. Better sensitivity was obtained using triethylamine (TEA) versus ammonium hydroxide, borate, or ammonium bicarbonate buffers. Derivatization of INH in tissues using TMPP did not appear as promising as *trans*-cinnamaldehyde, although extensive optimization was not performed. *trans*-Cinnamaldehyde was used for derivatization of INH in subsequent tissue analysis because of its ease of use and improved sensitivity compared with the other derivatization reagents.

The structures of INH, CA, and the INH-CA product are shown in Scheme 1. The carbonyl of cinnamaldehyde forms a stable Schiff base with the hydrazide moiety of INH resulting in an INH-CA compound of $[M + H]^+ = 252.1$. This derivative forms quickly; CA vapor from INH-CA standards spotted on MALDI plates readily derivatized INH in nearby target wells. MS/MS of the derivative at *m/z* 252 produces three main fragment ions at *m/z* 225, 123, and 80 as shown in Figure 2a. No significant signals were observed from the matrix or cinnamaldehyde itself at these transitions (Figure 2b). Thus, chemical background from these compounds is quite low.

Reagent Precoated Targets

CA was initially applied to tissues by two techniques. In one, tissues mounted on MALDI target plates were spray-coated with a CA solution (10 mM) using a TLC reagent sprayer. In this case, the CA contacted the tissue as a liquid, and several coatings were applied over time. In the second method, CA was applied to MALDI target plates (via a spin-coating technique), allowed to dry, and tissue sections were subsequently thaw-mounted on the CA-coated target. Although CA is a liquid at room temperature, crystals formed on the target plates, likely due to partial oxidation to *trans*-cinnamic acid [52]. Presumably enough unoxidized CA remains in the crystals to react with the INH, as the oxidized form would not be expected to form the derivative. Nuclear magnetic resonance (NMR) analysis of a dried coating indicated that approximately 1:1 CA:cinnamic acid was present. Subsequent studies have shown that a mixture of ~1:1 *trans*-cinnamaldehyde:*trans*-cinnamic acid may be directly applied to MALDI target plates. These plates readily produce uniform coatings without overnight drying/oxidation. In addition, this mixture has been applied by spray coating either manually using an artist airbrush or automatically using a robotic sprayer (TM Sprayer; HTX Technologies, LLC, Carrboro, NC, USA) with excellent results.

Tissues applied to plates spin-coated with CA generally gave ~10-fold more INH-CA signal than tissues that were spray-coated with the derivatization agent. While it is difficult to quantify the absolute amount of *trans*-cinnamaldehyde deposited onto the tissues with either method, based on the weight gained per plate following CA deposition (approximately 0.06 mg for spray coating and 60 mg for spin coating), there is approximately 1000× more CA present on a precoated target, thus providing a greater molar excess of CA compared to INH.

In order to more accurately determine the molar ratio of CA needed to effectively derivatize INH in tissues, various amounts of CA (50 to 5,000,000 pmol) were applied in discrete areas on dosed tissue sections (calculated to contain ~10 μg INH/g tissue or 70 pmol INH/mg tissue). CHCA matrix was applied on top of the CA spots. All spots were evaluated for the INH-CA derivative (*m/z* 252→80).

Approximately 500,000 pmol is required for maximum signal (Figure 3). This corresponds to a molar ratio of roughly 250,000:1 (assuming the tissue section is 1 mg and roughly 8 × 15 mm = 120 mm^2 and the area under the matrix spot is 3.14 mm^2 resulting in ~2 pmol INH/spot). At higher molar ratios, the INH-CA signals are lower, possibly because the increased amount of CA alters crystallization of CHCA or causes signal suppression. For premixed solutions a molar ratio of CA:INH of ~100 appears to be optimum (data not shown) suggesting that tissue contains compounds that may react or interfere with CA derivatization of INH. Based on these results, it is likely the precoated targets contain enough CA to successfully derivatize the INH present in tissues from dosed animals.

Due to the lack of sufficient INH-dosed lung tissue, we were unable to conduct additional studies of tissue thickness versus derivatization. Studies using rabbit liver (3, 6, 12 μm) showed relative INH-CA intensities of 2, 1.5, 1, respectively, indicating better derivatization with thinner tissue. However, it is difficult to section unembedded lung tissues thinly without extensive tearing and folding. Thus, all lung tissues were sectioned at 12 μm, but because all lung tissues in this study were processed identically, direct comparison among these tissues is reasonable.

Imaging MS/MS Analysis of INH-CA in Rabbit Lung Tissues

A series of lung tissues from rabbits dosed with INH and sacrificed at various time points, as well as two non-dosed control tissues, were thaw-mounted onto a target plate that was precoated with CA as described. CHCA matrix was applied and the tissues were analyzed via MS/MS of *m/z* 252. Data were acquired as one file over all of the tissue sections. There

is virtually no endogenous background in control tissue at the three major fragment masses (*m/z* 225, 123, and 80) as shown in Figure 4a. The transition *m/z* 252→80 was chosen for image reconstruction, however, reconstructed ion images for *m/z* 123 and 225 were similar. As shown in Figure 4b, INH is detected in all of the dosed rabbit tissues up to ~17 h post-dose, while no significant signal is observed in the non-dosed control lung tissue. The time-course clearly shows an accumulation of INH at the early time points followed by a reduction of signal with time as the drug is cleared from the body. The T_{max} (time to maximum serum concentration) for INH has been found to be 1 h or less and the $t_{1/2}$ (the half-life or rate of clearance) is 1 h to 1 h 30 min in rabbits (Via, Dartois, unpublished).

No significant localization of INH to either the unaffected lung tissue or lesion area was observed. For example, Figure 4c shows the H&E stained serial section for lung tissue from the 1 h 5 min rabbit as well as an expanded view of the MALDI ion image for the section analyzed in Figure 4b. Lesions are shown as dark purple regions (indicated by arrows) and the center one measures >1000 μm. As shown in the MALDI image, the INH-CA product is uniformly distributed over the tissue and no observable localization either to visually normal lung or granuloma is observed. The uniform distribution is not likely a result of any analyte delocalization; no significant INH-CA signal appears on the MALDI target outside of the tissue borders. However, the tissues evaluated in this study did not have large granulomas, therefore a more thorough assessment may be necessary using tissues from animals dosed with high concentrations of INH that also contain a number of larger lesions.

Correlation of MALDI MS/MS and HPLC-MS/MS Data

Absolute quantitation of INH in the tissue sections was not attempted via MALDI MS. The goal of the current study was to detect INH in tissue sections (via derivatization in this case) by IMS and evaluate localization of drug in unaffected lung tissue compared to TB lesion areas. However, it is reasonable to expect the signal response to be a function of drug concentration [11, 53]. Therefore, the MALDI LTQ response for INH-CA from the current rabbit study was compared with the results obtained by HPLC-MS/MS. The comparison is shown in Figure 5. Each time point represents a different animal that was evaluated by both MALDI and HPLC-MS/MS. The concentration of INH in unaffected lung tissue as determined by HPLC-MS/MS is expressed as ng INH/g tissue while the MALDI results are INH-CA signal intensities (*m/z* 252→ 80) from tissues shown in Figure 4 (average of 150 scans from each tissue section). For direct comparison, both values were converted into percent of maximum response. MALDI data were obtained from tissue located in only one area of the lung (for example, right upper lobe) while the HPLC data are averages of multiple lung areas ($n = 2–4$) and not always from the same area as that taken for MALDI analysis. Therefore, some variability is expected (calculated %RSDs range from 3 to 70 for HPLC lung results). Excised granulomas were also analyzed by HPLC-MS/MS for INH, and showed a similar trend (data not shown). Overall, no major differences in lung versus lesion concentrations of INH are noted with either HPLC-MS/MS or MALDI IMS. However, data do show that as the amount of drug in tissue decreases (as determined by HPLC-MS/MS) the MALDI MS/MS signal decreases; thus the trends observed for the two techniques are largely similar.

Conclusions

In-tissue derivatization has been shown to improve the detection of INH in cases where the analysis is hindered by isobaric interferences. High-resolution analysis may be used to distinguish isobaric species, however, this capability is not always available and may not improve the analysis if sensitivity is also an issue. For these instances, chemical derivatization is a viable alternative. For low molecular weight analytes, derivatization should ideally shift the molecular weight into a less complex spectral region (e.g., away

from MALDI matrix ions and low mass contaminants). Sensitivity may be enhanced by using a derivatizing agent with a fixed charge (e.g., TMPP or Girard's T). We found, as anticipated, that the total amount of reagent required for derivatization on tissue was significantly greater than for an equivalent amount of analyte in solution. This is due to the presence of many additional endogenous reactive sites in tissue. Precoating the MALDI target allows the necessary amount of reagent to be homogenously deposited while minimizing analyte delocalization.

Acknowledgments

The authors acknowledge support for this work (in part) by the Bill and Melinda Gates Foundation Accelerator grant N01 HD23342, (in part) by NIH/NIGMS grant 5R01 GM58008, and (in part) by the Intramural Research Program of NIAID, NIH. The assistance of Dr. Joey C. Latham, Dr. Kenneth E. Schriver, and Jamie Allen (Vanderbilt) and Danielle Weiner and Jacqueline Gonzales (NIH) is gratefully acknowledged.

References

1. Caprioli RM, Farmer TB, Gile J. Molecular imaging of biological samples: localization of peptides and proteins using MALDI-TOF MS. Anal Chem. 1997; 69(23):4751–4760. [PubMed: 9406525]
2. Stoeckli M, Chaurand P, Hallahan DE, Caprioli RM. Imaging mass spectrometry: A new technology for the analysis of protein expression in mammalian tissues. Nat Med. 2001; 7(4):493–496. [PubMed: 11283679]
3. Chaurand P, Sanders ME, Jensen RA, Caprioli RM. Proteomics in diagnostic pathology: profiling and imaging proteins directly in tissue sections. Am J Pathol. 2004; 165(4):1057–1068. [PubMed: 15466373]
4. Burnum KE, et al. Imaging mass spectrometry reveals unique protein profiles during embryo implantation. Endocrinology. 2008; 149(7):3274–3278. [PubMed: 18403475]
5. Stoeckli M, Staab D, Staufenbiel M, Wiederhold KH, Signor L. Molecular imaging of amyloid β peptides in mouse brain sections using mass spectrometry. Anal Biochem. 2002; 311:33–39. [PubMed: 12441150]
6. Andersson M, Groseclose MR, Deutch AY, Caprioli RM. Imaging mass spectrometry of proteins and peptides: 3D volume reconstruction. Nat Methods. 2008; 5(1):101–108. [PubMed: 18165806]
7. Hankin JA, Barkley RM, Murphy RC. Sublimation as a method of matrix application for mass spectrometric imaging. J Am Soc Mass Spectrom. 2007; 18(9):1646–1652. [PubMed: 17659880]
8. Burnum KE, et al. Spatial and temporal alterations of phospholipids determined by mass spectrometry during mouse embryo implantation. J Lipid Res. 2009; 50(11):2290– 2298. [PubMed: 19429885]
9. Garrett TJ, Yost RA. Analysis of intact tissue by intermediate-pressure MALDI on a linear ion trap mass spectrometer. Anal Chem. 2006; 78 (7):2465–2469. [PubMed: 16579637]
10. Troendle FJ, Reddick CD, Yost RA. Detection of pharmaceutical compounds in tissue by matrix-assisted laser desorption/ionization and laser desorption/chemical ionization tandem mass spectrometry with a quadrupole ion trap. J Am Soc Mass Spectrom. 1999; 10(12):1315–1321.
11. Reyzer ML, Hsieh Y, Ng K, Korfmacher WA, Caprioli RM. Direct analysis of drug candidates in tissue by matrix-assisted laser desorption/ionization mass spectrometry. J Mass Spectrom. 2003; 38:1081–1092. [PubMed: 14595858]
12. Khatib-Shahidi S, Andersson M, Herman JL, Gillespie TA, Caprioli RM. Direct molecular analysis of whole-body animal tissue sections by imaging MALDI mass spectrometry. Anal Chem. 2006; 78(18):6448–6456. [PubMed: 16970320]
13. Seeley EH, Oppenheimer SR, Mi D, Chaurand P, Caprioli RM. Enhancement of protein sensitivity for MALDI imaging mass spectrometry after chemical treatment of tissue sections. J Am Soc Mass Spectrom. 2008; 19(8):1069–1077. [PubMed: 18472274]
14. Grey AC, Chaurand P, Caprioli RM, Schey KL. MALDI imaging mass spectrometry of integral membrane proteins from ocular lens and retinal tissue. J Proteome Res. 2009; 8(7):3278–3283. [PubMed: 19326924]

15. Chaurand P, Norris JL, Cornett DS, Mobley JA, Caprioli RM. New developments in profiling and imaging of proteins from tissue sections by MALDI mass spectrometry. J Proteome Res. 2006; 5(11):2889–2900. [PubMed: 17081040]
16. Lemaire R, et al. MALDI-MS direct tissue analysis of proteins: Improving signal sensitivity using organic treatments. Anal Chem. 2006; 78 (20):7145–7153. [PubMed: 17037914]
17. Wang HYJ, Jackson SN, McEuen J, Woods AS. Localization and analyses of small drug molecules in rat brain tissue sections. Anal Chem. 2005; 77(20):6682–6686. [PubMed: 16223256]
18. Cornett DS, Frappier SL, Caprioli RM. MALDI-FTICR imaging mass spectrometry of drugs and metabolites in tissue. Anal Chem. 2008; 80 (14):5648–5653. [PubMed: 18564854]
19. Blau, K.; King, GS., editors. Handbook of Derivatives for Chromatography. Heyden and Son, Ltd; London: 1977. p. 576
20. Knapp, DR., editor. Handbook of Analytical Derivatization Reactions. John Wiley and Sons, Inc; New York: 1979. p. 741
21. Liu X, Qiu H, Lee RK, Chen W, Li J. Methylamidation for sialoglycomics by MALDI-MS: A facile derivatization strategy for both a2,3- and a2,6-linked sialic acids. Anal Chem. 2010; 82(19): 8300–8306. [PubMed: 20831242]
22. Rohmer M, et al. 3-aminoquinoline acting as matrix and derivatizing agent for MALDI MS analysis of oligosaccharides. Anal Chem. 2010; 82(9):3719–3726. [PubMed: 20387804]
23. Lin C, Hung WT, Chen CH, Fang JM, Yang WB. A new naphthimidazole derivative for saccharide labeling with enhanced sensitivity in mass spectrometry detection. Rapid Commun Mass Spectrom. 2010; 24:85–94. [PubMed: 19960495]
24. Xie J, et al. Extraction and derivatization in single drop coupled to MALDI-FTICR-MS for selective determination of small molecule aldehydes in single puff smoke. Anal Chim Acta. 2009; 638(2):198–201. [PubMed: 19327460]
25. Durairaj A, Limbach PA. Matrix-assisted laser desorption/ionization mass spectrometry screening for pseudouridine in mixtures of small RNAs by chemical derivatization, RNase digestion and signature products. Rapid Commun Mass Spectrom. 2008; 22:3727–3734. [PubMed: 18973194]
26. Li J, et al. Enhanced detection of thiol peptides by matrix-assisted laser desorption/ionization mass spectrometry after selective derivatization with a tailor-made quaternary ammonium tag containing maleimidyl group. Rapid Commun Mass Spectrom. 2007; 21:2608–2612. [PubMed: 17659650]
27. Snovida SI, Chen VC, Perreault H. Use of a 2,5-dihydroxybenzoic acid/aniline MALDI matrix for improved detection and on-target derivatization of glycans: a preliminary report. Anal Chem. 2006; 78(24):8561–8568. [PubMed: 17165854]
28. Ullmer R, Plematl A, Rizzi A. Derivatization by 6-aminoquinolyl-N-hydroxysuccinimidyl carbamate for enhancing the ionization yield of small peptides and glycopeptides in matrix-assisted laser desorption/ionization and electrospray ionization mass spectrometry. Rapid Commun Mass Spectrom. 2006; 20:1469–1479. [PubMed: 16586471]
29. Khan MA, et al. Analysis of derivatised steroids by matrix-assisted laser desorption/ionisation and post-source decay mass spectrometry. Steroids. 2006; 71(1):42–53. [PubMed: 16199070]
30. Sekiya S, Wada Y, Tanaka K. Derivatization for stabilizing sialic acids in MALDI-MS. Anal Chem. 2005; 77(15):4962–4968. [PubMed: 16053310]
31. Franck J, El Ayed M, Wisztorski M, Salzet M, Fournier I. On-tissue N-terminal peptide derivatizations for enhancing protein identification in MALDI mass spectrometric imaging strategies. Anal Chem. 2009; 81 (20):8305–8317. [PubMed: 19775114]
32. Vorm O, Roepstorff P, Mann M. Improved resolution and very high sensitivity in MALDI TOF of matrix surfaces made by fast evaporation. Anal Chem. 1994; 66(19):3281–3287.
33. Zhang H, Caprioli RM. Capillary electrophoresis combined with matrix-assisted laser desorption/ ionization mass spectrometry; continuous sample deposition on a matrix-precoated membrane target. J Mass Spectrom. 1996; 31(9):1039–1046. [PubMed: 8831154]
34. Wall DB, et al. Continuous sample deposition from reversed-phase liquid chromatography to tracks on a matrix-assisted laser desorption/ionization precoated target for the analysis of protein digests. Electrophoresis. 2002; 23(18):3193–3204. [PubMed: 12298091]
35. Grove K, Frappier S, Caprioli R. Matrix precoated MALDI MS targets for small molecule imaging in tissues. J Am Soc Mass Spectrom. 2011; 22(1):192–195. [PubMed: 21472558]

36. Peloquin CA. Pharmacology of the antimycobacterial drugs. Med Clin North Am. 1993; 77(6): 1253–1262. [PubMed: 8231410]
37. Jindani A, Dore CJ, Mitchison DA. Bactericidal and sterilizing activities of antituberculosis drugs during the first 14 days. Am J Respir Crit Care Med. 2003; 167(10):1348–1354. [PubMed: 12519740]
38. Mitchison DA. The search for new sterilizing anti-tuberculosis drugs. Front Biosci. 2004; 9:1059–1072. [PubMed: 14977529]
39. Young DB, Perkins MD, Duncan K, Barry CE III. Confronting the scientific obstacles to global control of tuberculosis. J Clin Invest. 2008; 118(4):1255–1265. [PubMed: 18382738]
40. Seifart HI, Gent WL, Parkin DP, van Jaarsveld PP, Donald PR. High-performance liquid chromatographic determination of isoniazid, acetylisoniazid and hydrazine in biological fluids. J Chromatogr B. 1995; 674(2):269–275.
41. Kim M, Stewart JT. HPLC post-column derivatization of aromatic amines using N-methyl-9-chloroacridinium triflate. Microchim Acta. 1990; 102(4):221–232.
42. Driouich R, Takayanagi T, Mitsuko O, Motomizu S. Investigation of salicylaldehyde-5-sulfonate as a precolumn derivatizing agent for the determination of n-alkane diamines, lysine, diaminopimelic acid, and isoniazid by capillary zone electrophoresis. J Pharmaceut Biomed Anal. 2003; 30(5):1523–1530.
43. Horikawa R, Tanimura T, Tamura Z. Method for fluorescence detection in the high-performance liquid chromatography of δ4-3-ketosteroids. J Chromatogr A. 1979; 168(2):526–529.
44. Cohen SA, Michaud DP. Synthesis of a fluorescent derivatizing reagent, 6-aminoquinolyl-N-hydroxysuccinimidyl carbamate, and its application for the analysis of hydrolysate amino acids via high-performance liquid chromatography. Anal Biochem. 1993; 211(2):279–287. [PubMed: 8317704]
45. Huang ZH, Shen T, Wu J, Gage DA, Watson JT. Protein sequencing by matrix-assisted laser desorption ionization-postsource decay-mass spectrometry analysis of theN-Tris(2,4,6-trimethoxyphenyl) phosphine-acetylated tryptic digests. Anal Biochem. 1999; 268(2):305–317. [PubMed: 10075821]
46. Via LE, et al. Tuberculous granulomas are hypoxic in guinea pigs, rabbits, and nonhuman primates. Infect Immun. 2008; 76(6):2333–2340. [PubMed: 18347040]
47. Fang PF, et al. Simultaneous determination of isoniazid, rifampicin, levofloxacin in mouse tissues and plasma by high performance liquid chromatography-tandem mass spectrometry. J Chromatogr B. 2010; 878(24):2286–2291.
48. Wang A, et al. HPLC–MS analysis of isoniazid in dog plasma. Chromatographia. 2007; 66(9):741–745.
49. Ng KY, et al. Quantification of isoniazid and acetylisoniazid in rat plasma and alveolar macrophages by liquid chromatography-tandem mass spectrometry with on-line extraction. J Chromatogr B. 2007; 847(2):188–198.
50. Song SH, et al. Simultaneous determination of first-line anti-tuberculosis drugs and their major metabolic ratios by liquid chromatography/tandem mass spectrometry. Rapid Commun Mass Spectrom. 2007; 21(7):1331–1338. [PubMed: 17340570]
51. Huang L, et al. Development and validation of a hydrophilic interaction liquid chromatography-tandem mass spectrometry method for determination of isoniazid in human plasma. J Chromatogr B. 2009; 877 (3):285–290.
52. Pound AW, Pound JR. The oxidation of cinnamaldehyde. J Phys Chem. 1934; 38:1045–1049.
53. Reich RF, Cudzilo K, Levisky JA, Yost RA. Quantitative MALDI-MS(*n*) analysis of cocaine in the autopsied brain of a human cocaine user employing a wide isolation window and internal standards. J Am Soc Mass Spectrom. 2010; 21(4):564– 571. [PubMed: 20097576]

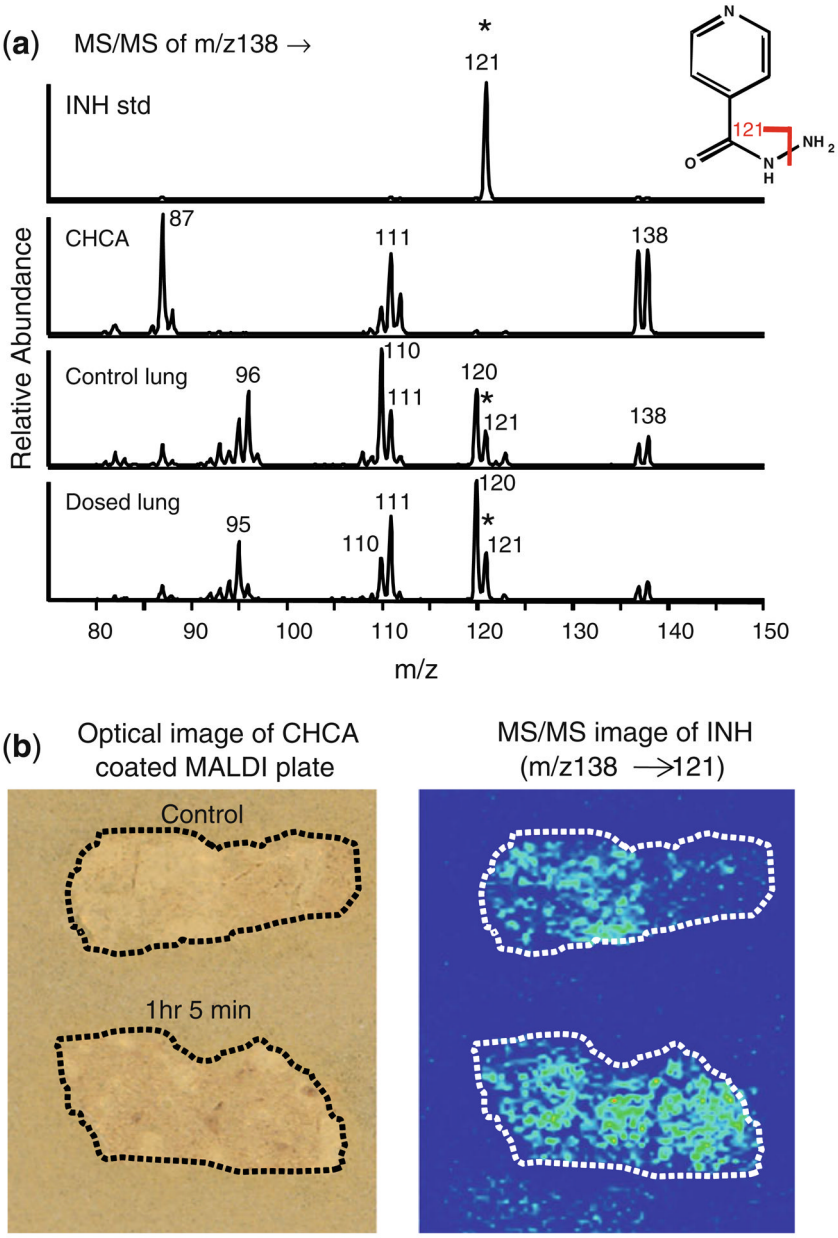

Figure 1.

Analysis of underivatized INH in rabbit lung tissue. The animal was dosed with rifampin/isoniazid/pyrazinamide/moxifloxacin at 30/50/125/25 mg/kg/d for 1 wk and sacrificed 1 h 5 min after the final dose. Non-INH dosed control tissue was also analyzed. **(a)** MS/MS spectra for INH (*m/z* 138→) from prepared standard (250 pmol on plate), CHCA blank, control lung, and dosed lung. **(b)** Optical image of rabbit tissue sections coated with CHCA (left) and reconstructed ion image of INH in rabbit tissues (right). The transition (*m/z* 138→121) was monitored. Due to endogenous background, it is not possible to distinguish dosed from control rabbit lung

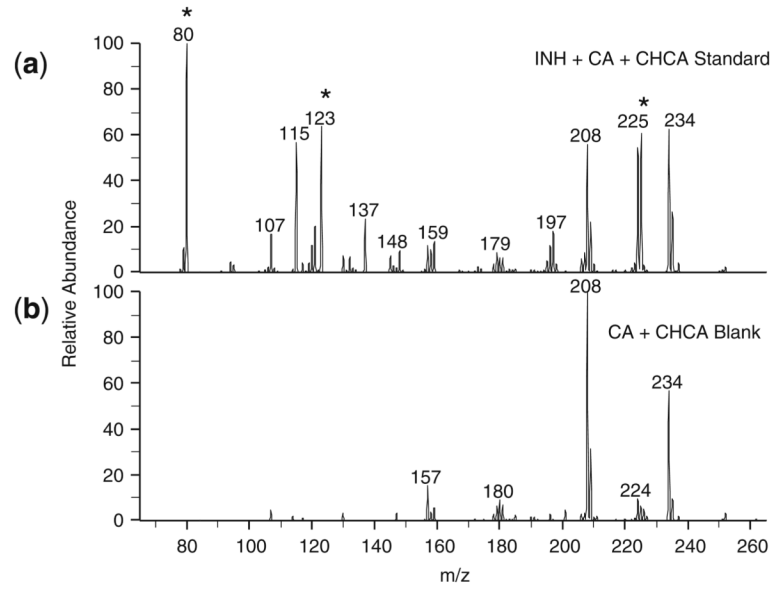

Figure 2.
MS/MS spectra for INH-CA derivative (*m/z* 252→) from (**a**) prepared standard (5 pmol on plate) (**b**) CA + CHCA blank

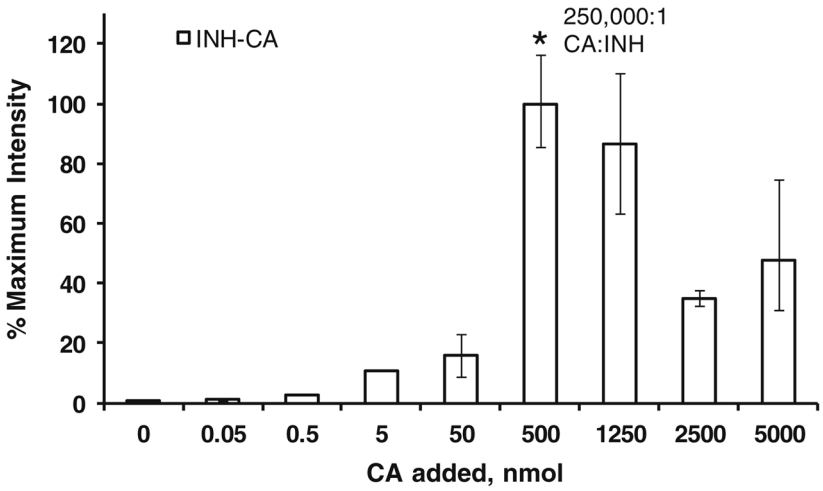

Figure 3.

The effect of CA:INH ratio on in situ derivatization of INH. Various amounts of CA (from 0 to 5000 nmol; $n = 2–4$) were added to dosed tissue calculated to contain ~70 pmol INH/mg tissue and the resulting CA derivative (m/z 252→80) was monitored. The optimum molar ratio was found to be ~250,000:1. Error bars indicate the highest and lowest values obtained, however, they are too small to be observed for values of 0–5 nmol

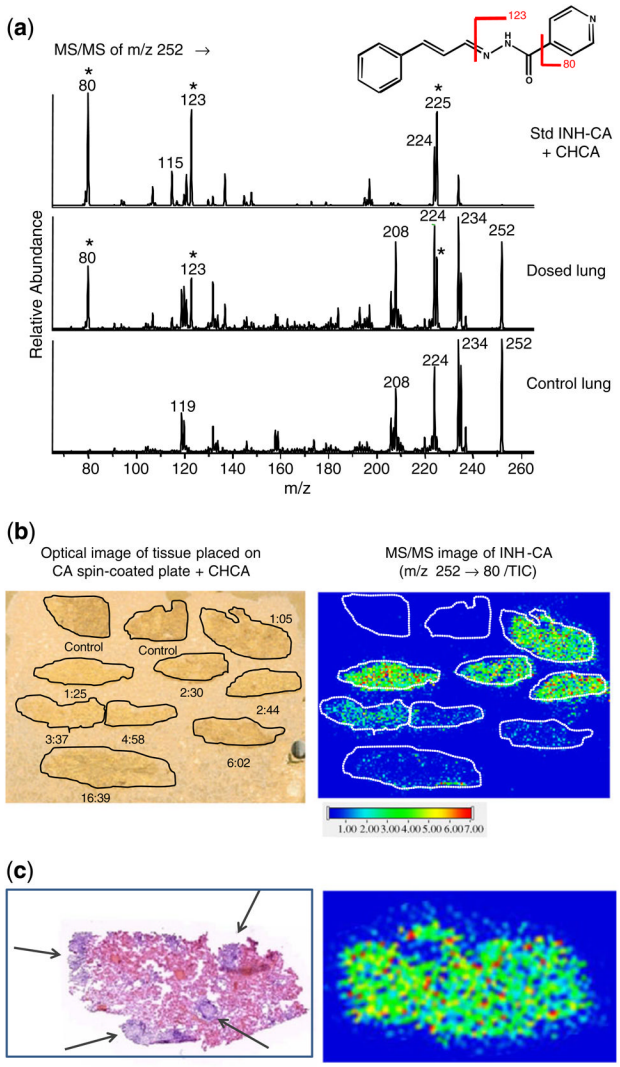

Figure 4.

Analysis of INH-CA derivative in rabbit lung tissue. Animals were dosed with rifampin/isoniazid/pyrazinamide/moxifloxacin at 30/50/125/25 mg/kg/d for 1 wk and sacrificed at various h:min after final dose. Non-INH dosed control tissues from two different rabbits were also analyzed. **(a)** MS/MS spectra for INH-CA derivative (*m/z* 252→) from prepared standard (125 pmol on plate), dosed lung from the image below (1 h 25 min), and control lung. **(b)** Optical image and MALDI image of rabbit tissues. Tissues were placed on targets that had been precoated with a layer of CA followed by CHCA deposition. The transition (*m/z* 252→80/total ion current) was used for ion image reconstruction. **(c)** H&E stained serial section for lung tissue from the 1 h 5 min rabbit and expanded view of the MALDI image from **(b)**. Lesions apparent as nuclei-rich dark purple areas (H&E) are indicated by arrows. This protocol allowed visualization of INH in dosed tissues up to ~17 h, with minimal interfering signal from the control tissue, however no localization to unaffected lung or lesion areas is observed

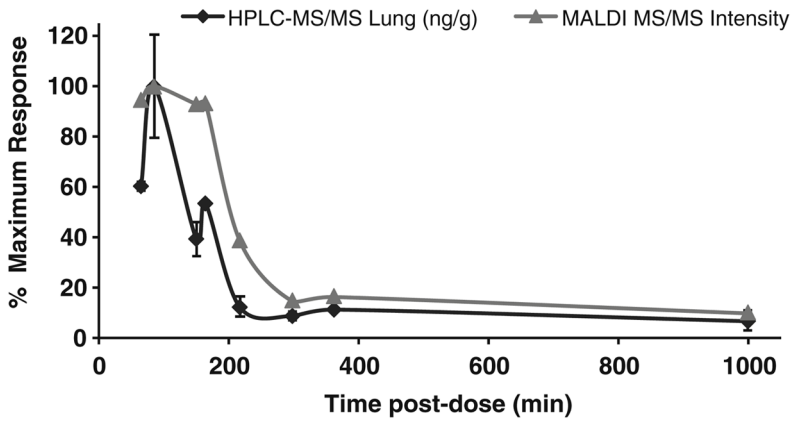

Figure 5.

Correlation of MALDI MS/MS and HPLC-MS/MS data. MALDI signal intensities (*m/z* 252→80) were obtained by averaging the intensity (150 scans) over each tissue shown in Figure 4, while HPLC-MS/MS results are an average of multiple areas of lung ($n = 2–4$). For direct comparison, each value was corrected to % of maximum response. HPLC-MS/MS variability noted by error bars ($\pm 1\sigma$) while MALDI data is from a single analysis. A similar trend is observed for both HPLC-MS/MS and MALDI MS/MS

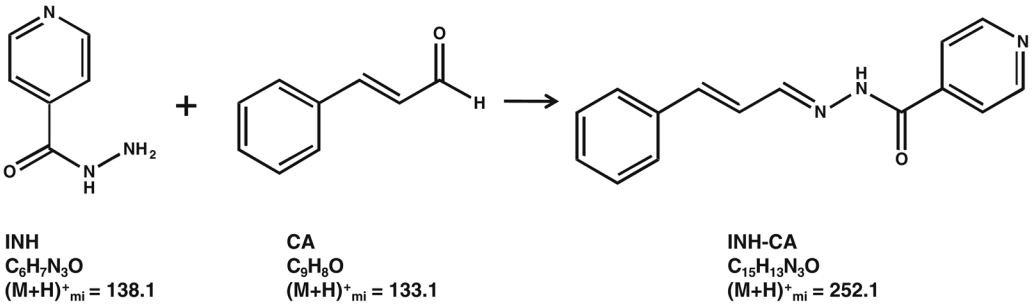

Scheme 1.
Structures of INH, CA, and INH-CA with monoisotopic molecular weights of protonated molecules

Table 1

Derivatization Reagents Evaluated for Isoniazid

Derivatizing agent	INH-derivative $[M + H]^+$ [a]	MS/MS fragments (*m/z*)[a]	Molar ratio deriv./INH	Solvent	~pH	Temp., °C[b]	Time, min[b]	Ref.
trans-Cinnamaldehyde	252.1	**80.0**, 122.9, 224.9	20	MeOH:H_2O	n/a	R.T.	10	19, 20, 40[c]
β-Phenylcinnamaldehyde	328.4	123.6, **137.5**, 148.5	20	MeOH:H_2O	n/a	R.T.	10	19, 20, 40
α-Bromocinnamaldehyde	330.3	137.5, 193.3, **250.3**	20	MeOH:H_2O	n/a	R.T.	60	19, 20, 40
4-Hydroxy-3-methoxycinnamaldehyde	298.3	138.5, **161.4**, 271.3	20	MeOH:H_2O	n/a	R.T.	10	19, 20, 40
4-Nitrocinnamaldehyde	297.3	**123.5**, 160.4, 175.4	20	MeOH:H_2O	n/a	R.T.	10	19, 20, 40
trans-4-(Diethylamino)cinnamaldehyde	323.4	106.7,**150.7**, 186.5	20	MeOH:H_2O	n/a	R.T.	10	19, 20, 40
Hydrocortisone	482.3	422.3, 452.3, **464.3**	20	MeOH:H_2O	n/a	R.T.	15	19, 43[c]
Waters AccQ-Fluor	308.2	137.9, **171.1**, 176.1	20	ACN:Borate or ACN:H_2O	8–9[d]	R.T.	15	44[e]
TMPP	710.2	573.2, 587.2, **591.2**	20	ACN:Borate or Ambic	8–9 [d]	55	>120	44, 45
TMPP	710.2	573.2, 587.2, **591.2**	2[f]	Triethylamine in ACN	7.5–8 [d]	55	120	31
TMPP	710.2	573.2, 587.2, **591.2**	20	NH_4OH in ACN[g]	9[d]	R.T.	>60	n/a

[a] Observed precursor mass and predominant fragments that were not present in CHCA blanks. Most abundant fragment ion is shown in bold. All derivatives produced $[M + H]^+$ except TMPP $[M]^+$.

[b] Temperature and time conditions used for ~complete derivatization of INH in solution.

[c] Recommended acidic conditions were tried but did not appear to be necessary in solution.

[d] pH measurements of equivalent concentration of modifier in aqueous solution.

[e] Also based on manufacturer's product instructions.

[f] Higher molar ratios produced reduced derivative signal.

[g] Low production of derivative (<5% of signal obtained using triethylamine in ACN).

MeOH = methanol; H_2O = water; ACN = acetonitrile; Ambic = ammonium bicarbonate; NH_4OH = ammonium hydroxide; R.T. = room temperature; Ref. = reference number

J Am Soc Mass Spectrom. Author manuscript; available in PMC 2012 August 22.